Hindawi
Shock and Vibration
Volume 2020, Article ID 8873701, 12 pages
https://doi.org/10.1155/2020/8873701

Research Article

Control and Stability Analysis of Double Time-Delay Active Suspension Based on Particle Swarm Optimization

Kaiwei Wu and Chuanbo Ren

School of Transportation and Vehicle Engineering, Shandong University of Technology, Zibo 255000, Shandong, China

Correspondence should be addressed to Chuanbo Ren; chuanbor@sdut.edu.cn

Received 29 March 2020; Revised 12 August 2020; Accepted 21 August 2020; Published 10 September 2020

Academic Editor: Mohammad Rafiee

With the application of an active control unit in the suspension system, the phenomenon of time delay has become an important factor in the control system. Aiming at the application of time-delay feedback control in vehicle active suspension systems, this paper has researched the dynamic behavior of semivehicle four-degree-of-freedom structure including an active suspension with double time-delay feedback control, focusing on analyzing the vibration response and stability of the main vibration system of the structure. The optimal objective function is established according to the amplitude-frequency characteristics of the system, and the optimal time-delay control parameters are obtained by using the particle swarm optimization algorithm. The stability for active suspension with double time-delay feedback control by frequency-domain scanning method is analyzed, and the simulation model of active suspension with double time delay based on feedback control is finally established. The simulation results show that the active suspension with double time-delay feedback control could reduce the body's vertical vibration acceleration, pitch acceleration, and other indicators significantly, whether under harmonic excitation or random excitation. So, it is indicating that the active suspension with double time-delay feedback control has a better control effect in improving the ride comfort of the car, and it has important reference value for further research on suspension performance optimization.

1. Introduction

With the rapid improvement of modern automobile technology, more and more consumers have higher requirements for car ride comfort and operational stability. In the overall structure of the car, the biggest relationship between comfort and operation stability is the suspension system of the car. Suspension, as a part of the elastic connection between the body and the axle, bears the force between the unsprung weight and the sprung weight, buffers the impact of road surface excitation on the body, and attenuates the vibration of various loads on the body. It is an important part of the vehicle. Compared with passive suspensions, active suspensions are highly adaptive [1, 2]. They can adjust the optimal damping in real time for the movement and road conditions of cars. Research on active suspension systems has become a focus in the field of vehicle engineering. With the application of the active control link, in the actual engineering system control, the control system needs a certain time from the signal collection and transmission, computer analysis, and response of the actuator, and time delay has become an inevitable factor in the suspension system control process [3].

Within this work, it is found that the time-delay control system has strong damping characteristics and high efficiency in the wide frequency bandwidth of the external excitations under the condition of system stability. In addition, the proposed controller requires external energy less than the control of stiffness and damping. Time delay has a great influence on the dynamic characteristics of the active suspension system and even leads to the instability of the feedback control system [4]. However, designing effective time delay and feedback gain can make the main system get a good damping effect. Many scholars have done a lot of research on the time-delay problem in vibration control systems. For example, Olgac et al. [5, 6] proposed a time-

delay dynamic vibration absorber and started a series of basic researches, namely installing a shock absorber with time-delay displacement feedback on the main vibration system. Vyhlidal et al. [7] studied and analyzed the stability of acceleration-feedback time-delay dynamic vibration absorber in the full time-delay region by using spectral analysis method and provided an effective method for the design of vibration absorber. Hu and Wang [8, 9] in order to analyze the stability interval of the time-delay dynamical system, used the stability switching idea to study the influence of the time-delay positive feedback on the system; Su and Tang [10, 11] studied the design of active suspension vibration controller with time delay by using the quarter-car model under random excitation; Xu and Li [12, 13, 14] studied the dynamic behavior of two-degree-of-freedom structure with time delay by using a direct method and analyzed the dynamic characteristics and stability of the system. Under the premise of ensuring stability, the vibration response of the main system was obtained through simulation; Saeed et al. [15–18] studied the influence of time delay on the control system dynamics and obtained the time-delay stability region. Then they applied the time-delay feedback control to the vibration control of the Jeffcott-rotor system and performed a numerical simulation. The simulation results show that time-delay feedback control can effectively suppress system vibration. From the existing research, the time-delay control despite the vibration analysis method has made great development; most of these studies are the work of the basic theory of the structure with few degrees of freedom. The suspension system of the vehicle is a very complex multi-degree of freedom vibration system with many uncertainties and complexities. For the quarter-car model with single time-delay feedback control, although the model is simple, the dynamic response obtained is not comprehensive. The research on the stability of the delayed feedback system is not perfect, so this paper analyzes the dynamic response of a half-car four-degree-of-freedom suspension model with double time-delay feedback control under the premise of stability.

According to the dynamic characteristics of a four-degree-of-freedom half-vehicle suspension, this paper applies the active suspension theory with stable double time-delay feedback control to a half-vehicle model and innovates a frequency-domain scanning method to determine the stability interval of double time delay. The active suspension with double delay feedback control under random excitation is simulated.

2. Half-Care Mathematical Model

According to the characteristics of the vehicle suspension, the physical model of the vehicle suspension system is simplified from the perspective of scientific research. When the vehicle is symmetrical to its longitudinal axis, only the vertical vibration and pitch vibration of the vehicle body have the greatest impact on ride comfort, which is simplified as a two-axis four-degree-of-freedom physical model. m is the mass of the half-car body; I is the moment of inertia of the axis perpendicular to the centroid of the half-car model; m_{tf} is the unsprung mass of the front wheels; m_{tr} is the unsprung mass of the rear wheels; k_{sf} is the spring stiffness coefficient of the front suspension; k_{sr} is the spring stiffness coefficient of the rear suspension; c_{sf} is the damping of the front suspension coefficient; c_{sr} is the damping coefficient generated by the rear suspension; k_{tf} is the stiffness coefficient generated by the front tire; k_{tr} is the stiffness coefficient generated by the rear tire; φ is the longitudinal pitch angle of the half body of the vehicle; x_{tf}, x_{tr} are the mass displacement of front and rear sprung; x_{gf}, x_{gr} are the excitation displacement input of front and rear road surface; f_f, f_r are the active control force of the front and rear suspension; L_f, L_r are the distance from the front and rear suspension to the center of mass of the half-car; the model is shown in Figure 1.

According to Newton's second law, the dynamic differential equation of the half-car four-degree-of-freedom model can be obtained as follows [19]:

$$\begin{cases} m_{tf}\ddot{x}_{tf} - k_{sf}\left(x_{sf} - x_{tf}\right) - c_{sf}\left(\dot{x}_{sf} - \dot{x}_{tf}\right) + k_{tf}\left(x_{tf} - x_{gf}\right) + f_f = 0, \\ m_{tr}\ddot{x}_{tr} - k_{sr}\left(x_{sr} - x_{tr}\right) - c_{sr}\left(\dot{x}_{sr} - \dot{x}_{tr}\right) + k_{tr}\left(x_{tr} - x_{gr}\right) + f_r = 0, \\ m\ddot{x}_c + k_{sf}\left(x_{sf} - x_{tf}\right) + c_{sf}\left(\dot{x}_{sf} - \dot{x}_{tf}\right) - f_f + k_{sr}\left(x_{sr} - x_{tr}\right) + c_{sr}\left(\dot{x}_{sr} - \dot{x}_{tr}\right) - f_r = 0, \\ I\ddot{\varphi} - L_f\left[k_{sf}\left(x_{sf} - x_{tf}\right) + c_{sf}\left(\dot{x}_{sf} - \dot{x}_{tf}\right) - f_f\right] + L_r\left[k_{sr}\left(x_{sr} - x_{tr}\right) + c_{sr}\left(\dot{x}_{sr} - \dot{x}_{tr}\right) - f_r\right] = 0, \end{cases} \tag{1}$$

where $f_f = g_1 x_{tf}(t - \tau_1)$ and $f_r = g_2 x_{tr}(t - \tau_2)$ represent the active control force of front suspension and rear suspension, respectively; x_{gf} and x_{gr} are the excitation displacement input of the front and rear road surface, respectively; g_1 and g_2 are the time-delay feedback gain coefficients of the active control force of the front and rear suspensions, respectively; τ_1 and τ_2 are the time delay of the active control force of the front and rear suspensions, respectively.

As in Figure 1, when the pitch angle φ is small $\varphi \approx \tan\varphi$, the approximate values are as follows:

$$\begin{cases} x_{sf} = x_c - L_f\varphi, \\ x_{sr} = x_c + L_r\varphi. \end{cases} \tag{2}$$

Equations of motion (1) and (2) can be expressed as follows:

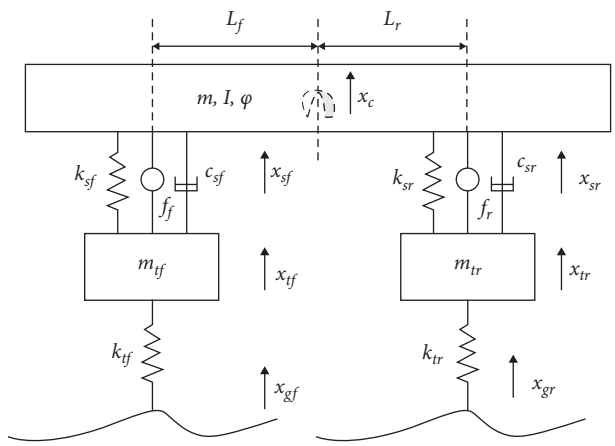

Figure 1: Four-degree-of-freedom suspension model with active control with double time- delay.

$$\begin{cases} \ddot{x}_{tf} = \dfrac{\left(k_{sf}\left(x_{sf} - x_{tf}\right) + c_{sf}\left(\dot{x}_{sf} - \dot{x}_{tf}\right) - k_{tf}\left(x_{tf} - x_{gf}\right) - f_f\right)}{m_{tf}}, \\ \ddot{x}_{tr} = \dfrac{\left(k_{sr}\left(x_{sr} - x_{tr}\right) + c_{sr}\left(\dot{x}_{sr} - \dot{x}_{tr}\right) - k_{tr}\left(x_{tr} - x_{gr}\right) - f_r\right)}{m_{tr}}, \\ \ddot{x}_c = \dfrac{\left(-k_{sf}\left(x_{sf} - x_{tf}\right) - c_{sf}\left(\dot{x}_{sf} - \dot{x}_{tf}\right) + f_f - k_{sr}\left(x_{sr} - x_{tr}\right) - c_{sr}\left(\dot{x}_{sr} - \dot{x}_{tr}\right) + f_r\right)}{m}, \\ \ddot{\varphi} = \dfrac{L_f\left[k_{sf}\left(x_{sf} - x_{tf}\right) + c_{sf}\left(\dot{x}_{sf} - \dot{x}_{tf}\right) - f_f\right] - L_r\left[k_{sr}\left(x_{sr} - x_{tr}\right) + c_{sr}\left(\dot{x}_{sr} - \dot{x}_{tr}\right) - f_r\right]}{I}. \end{cases} \tag{3}$$

3. Optimization Control Analysis of Suspension System

Figure 2 shows the amplitude-frequency characteristics of the body when the time- delay feedback control parameters are different. It can be seen from Figure 2 that when the time delay and the feedback gain are zero, the system reaches the highest point of amplitude at 5.9 Hz. This indicates that when the external excitation frequency is equal to the natural frequency of the system, the system is forced to vibrate at the maximum amplitude due to resonance effects. When the feedback control parameters are $\tau_{03} = 0.434$; $\tau_{02} = 0.452$; $gf_{01} = 19287$; $gr_{01} = 23930$, the system's vibration response decreases significantly around 5.9 Hz. This shows that the time-delay feedback control can attenuate vibration, and there must be a maximum damping point in a certain interval. When the feedback gain parameters are $\tau_{05} = 0.906$; $\tau_{06} = 0.546$; $gf_{02} = 25333$; $gr_{02} = 23371$, there are multiple peaks in the response curve of the system. This indicates that the presence of a time delay factor can also destabilize the system.

Through analysis, it can be seen that the time delay feedback control can change the vibration response of the system. Therefore, in this paper, the optimal time delay and feedback gain coefficient are obtained by particle swarm optimization, and the frequency-domain scanning method is used to ensure the stability of the time-delay feedback system, so as to achieve the best vibration reduction effect.

Fourier transform the dynamic differential equation of the half-car four-degree-of-freedom model, transform the time-domain characteristics to the frequency-domain range for research and analysis, and rewrite it into the form of a matrix. The Fourier change of equation (1) is as follows:

$$A_{44}X = B, \tag{4}$$

where $X = \left[X_c \;\; \varphi \;\; X_{tf} \;\; X_{tr}\right]^T$, $B = \left[(k_{tf}X_{gf}/m_{tf})0\,(k_{tr}X_{gr}/m_{tr})0\right]^T$, $X_{gr} = X_{gf}e^{-s\Delta t}$

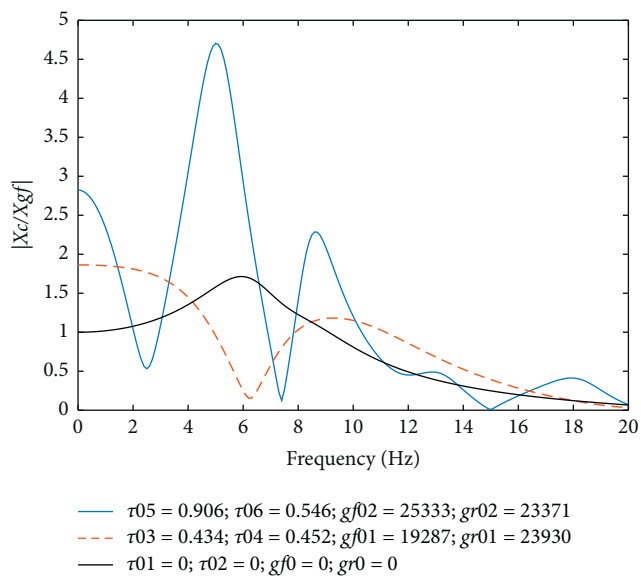

Figure 2: Amplitude-frequency response curve.

$$A44 = \begin{bmatrix} a_{11} & a_{12} & a_{13} & a_{14} \\ a_{21} & a_{22} & a_{23} & a_{24} \\ a_{31} & a_{32} & a_{33} & a_{34} \\ a_{41} & a_{42} & a_{43} & a_{44} \end{bmatrix},$$

$$\begin{aligned}
a_{11} &= -m_{tf}\omega^2 + i\omega c_{sf} + \left(k_{sf} + k_{tf}\right) + g_f e^{-i\tau_1\omega}, \\
a_{12} &= 0, a_{13} \\
a_{14} &= i\omega c_{sf} L_f + k_{sf} L_f, \\
a_{21} &= 0, a_{22} \\
a_{23} &= -k_{sr} - i\omega c_{sr}, \\
a_{24} &= k_{sr} L_r - i\omega c_{sr} L_r, \\
a_{31} &= -k_{sf} - i\omega c_{sf} - g_f e^{-i\omega\tau_1}, \\
a_{32} &= -k_{sr} - i\omega c_{sr} - g_r e^{-i\omega\tau_2}, \\
a_{33} &= -m_c\omega^2 + i\omega\left(c_{sf} + c_{sr}\right) + k_{sf} + k_{sr}, \\
a_{34} &= i\omega\left(c_{sr} L_r - c_{sf} L_f\right) + k_{sr} L_r - k_{sf} L_f, \\
a_{41} &= L_f\left(i\omega c_{sf} + k_{sf} + g_f e^{-i\omega\tau_1}\right), \\
a_{42} &= -L_r\left(i\omega c_{Sr} + k_{Sr} + g_r e^{-i\omega\tau_2}\right), \\
a_{43} &= -L_f\left(i\omega c_{sf} + k_{sf}\right) + L_r\left(i\omega c_{sr} + k_{sr}\right), \\
a_{44} &= -I\omega^2 + L_f^2\left(k_{sf} + i\omega c_{sf}\right) + L_r^2\left(i\omega c_{Sr} + k_{Sr}\right).
\end{aligned} \tag{5}$$

External excitation input to front and rear wheels has a time difference of Δt of $x_{gr}(t) = x_{gf}(t - \Delta t)$, where $\Delta t = (L_f + L_r)/v$.

In equation (4), the amplitude-frequency characteristic function $|H_{\dot{X}_c \sim \dot{X}_{gf}}(\omega)| = \omega|X_c(\omega)/X_{gf}(\omega)|$ of the vertical acceleration of the body centroid and the amplitude-frequency characteristic function $|H_{\ddot{\varphi}\sim\dot{X}_{gf}}(\omega)| = \omega|\varphi(\omega)/X_{gf}(\omega)|$ of the acceleration of the body pitch angle are obtained, respectively.

The vertical centroid acceleration of the vehicle body and the vertical pitch acceleration of the vehicle body are important indicators to measure the ride comfort of the vehicle. Therefore, the vertical acceleration of the center of mass of the vehicle body and the vertical acceleration angle of the vehicle body are used as the main evaluation indicators to establish a weighted objective function for the optimization of the control parameters. At the same time, according to the engineering background, the search range is set: the feedback gain is no more than twice the passive stiffness. The smaller the delay, the smaller the overshoot:

$$\min J\left(g_f, g_r, \tau_1, \tau_2\right) = n_1\left|H_{\ddot{X}_c} \sim \dot{X}_{gf}(\omega)\right| + n_2\left|H_{\ddot{\varphi}\sim\dot{X}_{gf}}(\omega)\right|,$$
$$s.t. \begin{cases} -2k \le g \le 2k, \\ 0 < \tau \le 1. \end{cases} \tag{6}$$

where the weighting coefficients n_1 and n_2 are 0.7 and 0.3, which measures the importance of each amplitude-frequency function in the objective function.

The objective function is optimized based on the established objective function and the characteristics of the particle swarm optimization algorithm [20]. Due to the large difference in the magnitude of the optimized feedback gain and time delay, a four-dimensional search space is assumed to represent the two feedback gains and time delays, respectively. The individual positions are updated by tracking individual extreme values Pbest and group extreme values Gbest. Once the position is updated, the fitness value is calculated. By comparing the fitness value of the new particle with the individual extreme value, the fitness value of the group extreme value updates the individual extreme value Pbest and the group extreme value Gbest position; in each iteration process the particle passes, the individual extreme value and group extreme value update their speed and position. The formula is updated to the following equation:

$$\begin{aligned}
V_{ik}^{k+1} &= \alpha V_{id}^k + \varepsilon_1 r_1\left(P_{id}^k - X_{id}^k\right) + \varepsilon_2 r_2\left(P_{gd}^k - X_{id}^k\right), \\
X_1^{k+1} &= X_{i1}^k + r V_{i1}^{k+1},
\end{aligned} \tag{7}$$

where α is the inertial weight, $d = 1, 2$; $i = 1, 2, \ldots, n$; k is the current iteration time, V_{id} is the particle update speed, ε_1 and ε_2 are nonnegative acceleration factor, r_1 and r_2 are generated from [0, 1] random constant. We select 60 particles for iterative optimization randomly in order to find the optimal individual extremum and group extremum more quickly during optimization, $\varepsilon_1 = \varepsilon_2 = 2$, after 200 iterations, we obtain the change graph of the number of iterations of the fitness function of the suspension performance index as in Figure 3. With reference to a vehicle's suspension parameters (as in Table 1), the global optimal control parameters under random excitation and harmonic excitation are obtained, respectively, after optimization: $g_f = 19345$N/m, $g_r = 26150$N/m, $\tau_1 = 0.5530\,s$, $\tau_2 = 0.5186\,s$; $g_{ff} = 29653$N/m, $g_{rr} = -4416$N/m, $\tau_{11} = 0.3255\,s$, $\tau_{22} = 0.5438\,s$.

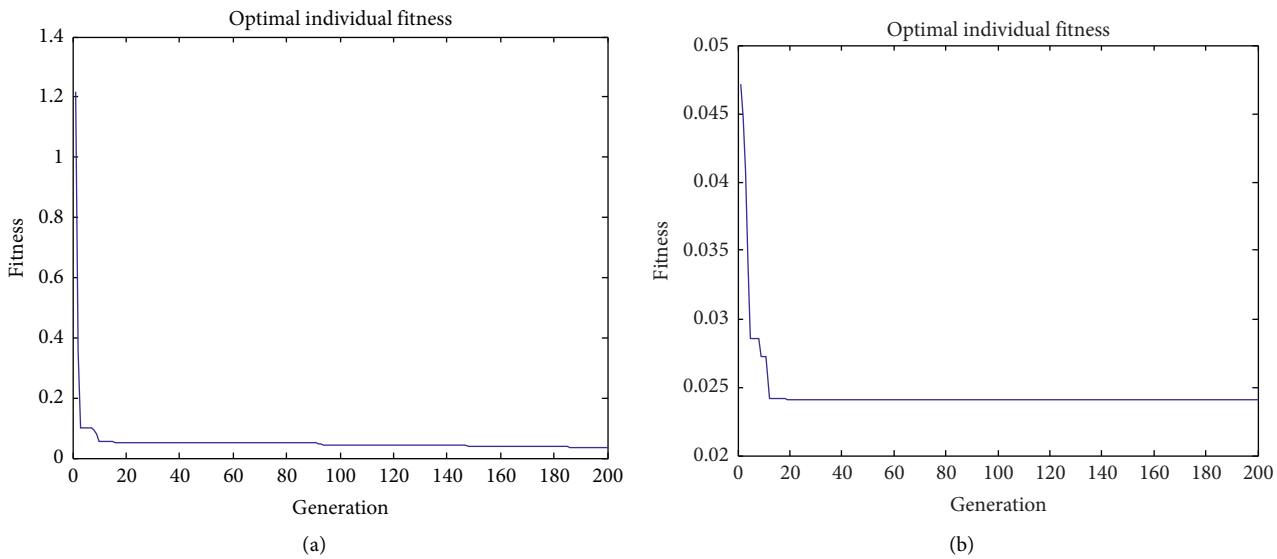

Figure 3: Iterative optimization of the fitness function. (a) The fitness function of optimization under harmonic excitation. (b) The fitness function of optimization under random excitation.

4. Stability Analysis

The existence of time delay has a great impact on the dynamic performance of the active suspension system. In order to ensure the stability of the feedback control system with double time delay, the frequency-domain scanning method is proposed in this paper to analyze the stability of the optimized control parameters [21–24].

First, equation (1) is rewritten as the form of state equation:

$$\dot{x}(t) = Ax(t) + Bx(t-\tau), \tag{8}$$

where A and B are constant matrices, and $\tau \geq 0$ is constant.

$$x = \left[x_{tf} \;\; \dot{x}_{tf} \;\; x_{tr} \;\; \dot{x}_{tr} \;\; x_c \;\; \dot{x}_c \;\; j \;\; \dot{j} \right]^T,$$

$$A = \begin{bmatrix} 0 & 1 & 0 & 0 & 0 & 0 & 0 & 0 \\ -k_{sf} + k_{tf}/m_{tf} & -c_{sf} + c_{sr}/m_{tf} & 0 & 0 & m_{sf}/m_{tf} & c_{sf}/m_{tf} & -L_f k_{sf}/m_{tf} & L_f c_{cf}/m_{tf} \\ 0 & 0 & 0 & 1 & 0 & 0 & 0 & 0 \\ 0 & 0 & -k_{sr} + k_{tr}/m_{tr} & -c_{sr}/m_{tr} & k_{sr}/m_{tr} & -c_{sr}/m_{tr} & L_r k_{sr}/m_{tr} & L_r c_{sr}/m_{tr} \\ 0 & 0 & 0 & 0 & 0 & 1 & 0 & 0 \\ k_{sf}/m & c_{sf}/m & k_{sr}/m & c_{sr}/m & -k_{sf} + k_{tf}/m & -c_{sf} + c_{sr}/m & L_f k_{sf} - L_r k_{sr}/m & L_f c_{sf} - L_r c_{sr}/m \\ 0 & 0 & 0 & 0 & 0 & 0 & 0 & 1 \\ -L_f k_{sf}/I & -L_f c_{cf}/I & L_r k_{sr}/I & L_r c_{sr}/I & L_f k_{sf} - L_r k_{sr}/I & L_f c_{sf} - L_r c_{sr}/I & -L_f^2 k_{sf} + L_r^2 K_{sr}/I & -L_f^2 c_{sf} + L_r^2 c_{sr}/I \end{bmatrix},$$

$$B = \begin{bmatrix} 0 & 0 & 0 & 0 & 0 & 0 & 0 & 0 \\ 1/m & 0 & 1/m & 0 & 0 & 0 & 0 & 0 \\ 0 & 0 & 0 & 0 & 0 & 0 & 0 & 0 \\ -l_f/I & 0 & l_f/I & 0 & 0 & 0 & 0 & 0 \\ 0 & 0 & 0 & 0 & 0 & 0 & 0 & 0 \\ -1/m_{tf} & 0 & 0 & 0 & 0 & 0 & 0 & 0 \\ 0 & 0 & 0 & 0 & 0 & 0 & 0 & 0 \\ 0 & 0 & -1/m_{tr} & 0 & 0 & 0 & 0 & 0 \end{bmatrix}. \tag{9}$$

Table 1: Vehicle suspension model parameters.

Vehicle parameters	Value
m/(kg)	690
I/(kgm^2)	1200
m_{tf}/(kg)	40.5
m_{tr}/(kg)	45.4
k_{tf} (k_{tr})/(N·m^{-1})	192000
k_{sf}/(N·m^{-1})	17000
k_{sr}/(N·m^{-1})	22000
L_f/(m)	1.25
L_r/(m)	1.51
c_{sf} (c_{sr})/(N·s·m^{-1})	1500

The characteristic equation of (1) of time-delay control system is as follows:

$$\det\left(sI - A - Be^{-\tau s}\right) = 0. \tag{10}$$

The specific form is as follows:

$$\mathrm{CE}(s,z) = a_n(s)z^n + a_{n-1}(s)z^{n-1} + \cdots + a_0(s) = \sum_{k=0}^{n} a_k(s)z^k = 0, \tag{11}$$

where

$$\begin{aligned} a_0 &= c_6s^6 + c_5s^5 + c_4s^4 + c_3s^3 + c_2s^2 + c_1s^1 + c_0, \\ a_1 &= c_6s^6 + c_5s^5 + c_4s^4 + c_3s^3 + c_2s^2 + c_1s^1 + c_0, \\ a_2 &= c_8s^8 + c_7s^7 + c_6s^6 + c_5s^5 + c_4s^4 + c_3s^3 + c_2s^2 + c_1s^1 + c_0. \end{aligned} \tag{12}$$

$z = e^{-\tau s}$; $n = 2$, c is the coefficient of the characteristic equation.

Furthermore, for a given $a_k(s)(k = 0, 1, \ldots, n)$, there exists a continuous polynomial of $G_l(s)(1 = 1, \cdots, n)$ that satisfies the system's equation of state that can be equivalent to the following:

$$\mathrm{CE}(s,z) = a_n(s)\prod_{l=1}^{n}\left(z + G_l(s)\right)^k, \tag{13}$$

where $a_n(s)$ is a constant, $G_l(s)$ satisfies the following:

$$\sum_{k=0}^{n}\left(\frac{a_k(s)}{a_n(s)}\right)\left(-G_l(s)\right)^k = 0. \tag{14}$$

It is not necessary to find polynomial $G_l(s)$, because s and z are complex numbers, $\mathrm{CE}(s,z) = 0$ if and only if a subquasipolynomial $(z + G_l(s))(1 = 1, \ldots, n)$ is equal to zero.

Calculate the time delay; substitute $s = w_{l,m}$ for $\mathrm{CE}(s,z) = 0$, calculate z at zero, choose the root of 1, $x + y_i$, by calculating the θ value in $e^{-i\theta} = x + y_i$, where $\theta = \arctan(-y/x) + 2\pi$, when $x > 0$, $y > 0$; the time delay is $\theta/w + 2r\pi/w\,(r = 0, 1, \ldots, \infty)$.

We made stability analysis of time-delay control parameters g_f, g_r, τ_1, and τ_2 under random excitation by frequency-domain scanning method. The control system is stable when the time delay is equal to zero (the characteristic roots of the equation are as follows).

$$\begin{aligned} \lambda_1 &= -2.026785791140518160853583130 6952 + 17.09055324096044661032605555 8861^{*}i, \\ \lambda_2 &= -18.70877436741678982244310607 5043 - 70.20574198581773837185501530 0647^{*}i, \\ \lambda_3 &= -37.27414377346723335112963091 8096 + 61.65780248358458787021613724 5193^{*}i, \\ \lambda_4 &= -18.70877436741678982244310607 5043 + 70.20574198581773837185501530 0647^{*}i, \\ \lambda_5 &= -2.121389667009275090694452823 0251 + 7.273177337780497085198001393 9354^{*}i, \\ \lambda_6 &= -2.026785791140518160853583130 6952 - 17.09055324096044661032605555 8861^{*}i, \\ \lambda_7 &= -2.121389667009275090694452823 0251 - 7.273177337780497085198001393 9354^{*}i, \\ \lambda_8 &= -37.27414377346723335112963091 8096 - 61.65780248358458787021613724 5193^{*}i. \end{aligned} \tag{15}$$

It can be obtained that the characteristic roots of the system are in the left half-plane of the complex plane. Therefore, the active suspension system with double time-delay feedback control at $\tau = 0$ is stable. Figure 4 shows the relationship between $|z|$ and w generated by the frequency-domain scanning method, The system has two crossover frequencies $w_1 = 20.7651$, $w_2 = 20.7653$. The system has two positive imaginary roots, corresponding to two subquasipolynomials, and the crossing directions of the two imaginary roots are from left to right. Thus, as the time delay increases, once the system has characteristic virtual roots, the system will no longer be stable; the system is asymptotically stable when $\tau_2 \in (0, 0.6312)$. Similarly, the stability analysis of the time-delay control parameters under harmonic excitation is performed, and the stability interval of the time delay is $\tau_3 \in (0, 0.5817)$.

5. Establishing a Simulation Model and Result Analysis

5.1. Simulation Analysis under Harmonic Excitation. Take the optimized double time-delay control parameters into

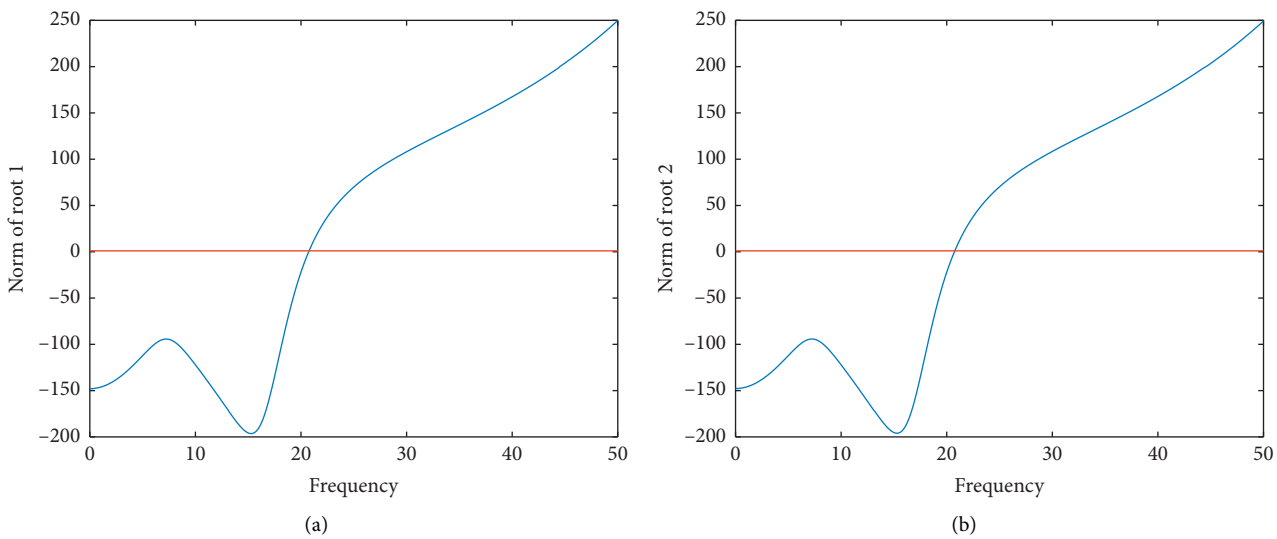

Figure 4: Modulus of Z in the characteristic equation. (a) Norm of root1. (b) Norm of root2.

equation (1). Taking the harmonic excitation $x_{gf} = 0.05\sin(7t)$ as the road input excitation, the vibration response characteristics of the vehicle in the time domain of the passive suspension system and the active suspension system with double time-delay feedback control are analyzed. We made a time-domain simulation of suspension body acceleration, pitch acceleration, suspension dynamic deflection, and tire dynamic displacement. The simulation curve is as in Figure 5:

The RMS value of the vehicle ride comfort index is calculated (as in Table 2) according to the 20 s simulation data. Compared with the passive suspension, Figures 5(a) and 5(b) give a comparison of body acceleration and body pitch acceleration response, respectively. The active suspension with double time-delay feedback control reduces the body's center of mass acceleration and pitch acceleration significantly. The RMS value drops from 3.0647 and 2.3646 to 0.5026 and 1.1162, and the damping efficiency is as high as 83.60% and 52.80%. It can be seen from Figures 5(c) and 5(d) that the dynamic deflection of the front and rear suspensions has also been reduced significantly. The RMS values have decreased from 0.0383 and 0.0772 to 0.0275 and 0.0362 correspondingly, and the damping efficiency is as high as 9.78% and 28.20%. It can be seen from (e) and (f) of Figure 5 that the front and rear tire dynamic relative displacements have also been reduced significantly, and the corresponding RMS value of the tire dynamic displacements have decreased from 0.0108 and 9.7508e − 4 to 0.0020 and 3.3363e − 4. It dropped by 81.48% and 68.78%. The simulation results show that the active suspension system with double time-delay feedback control reduces the body acceleration and pitch acceleration without increasing the tire deformation and dynamic load, ensuring the safety of vehicle driving and vehicle handling stability. This shows the effectiveness of the active control method with double time delay under harmonic excitation.

5.2. Simulation Analysis under Random Excitation. In order to further study the damping effect of active suspension with double time-delay feedback control, the time-delay parameters optimized by particle swarm optimization in this paper are applied to the vehicle active suspension model with double time delay in the actuator. In order to verify the damping effect of active suspensions with double time delay, the vehicle is simulated to travel at a speed of 20 m/s. The parameters of an automobile suspension system are shown in Table 1. Random excitation is selected as the vertical disturbance to the wheel axle. Here, a sine function superposition method is used to establish a time-domain model of random excitation as in Figure 6:

$$x_r(t) = \sum_{i=1}^{n} \xi_i \sin(\omega_i t + \delta_i), \tag{16}$$

where ξ is the amplitude, ω is the equivalent frequency, and δ is the value randomly distributed on $(0, 2\pi)$.

The optimized parameters are brought into equation (1), and the random excitation is selected as the vertical disturbance to the wheel and shaft to analyze the vibration response characteristics of the vehicle in the time-domain state of the passive suspension system and the active suspension system with double time-delay feedback control. Time-domain simulation is performed for the body acceleration, pitching acceleration, suspension dynamic deflection, and tire dynamic displacement of the suspension, and the simulation curves are as in Figure 7.

From the time-domain simulation in Figure 7 and the root mean square value of the vehicle ride comfort index calculated from the 20 s simulation data as in Table 3, compared with the passive suspension, the body acceleration and pitch acceleration are as in Figures 7(a) and 7(b). Corresponding comparison graphs are given, respectively, and their corresponding root mean square values have dropped from 1.4898 and 2.3858 to 1.2578 and 1.8610,

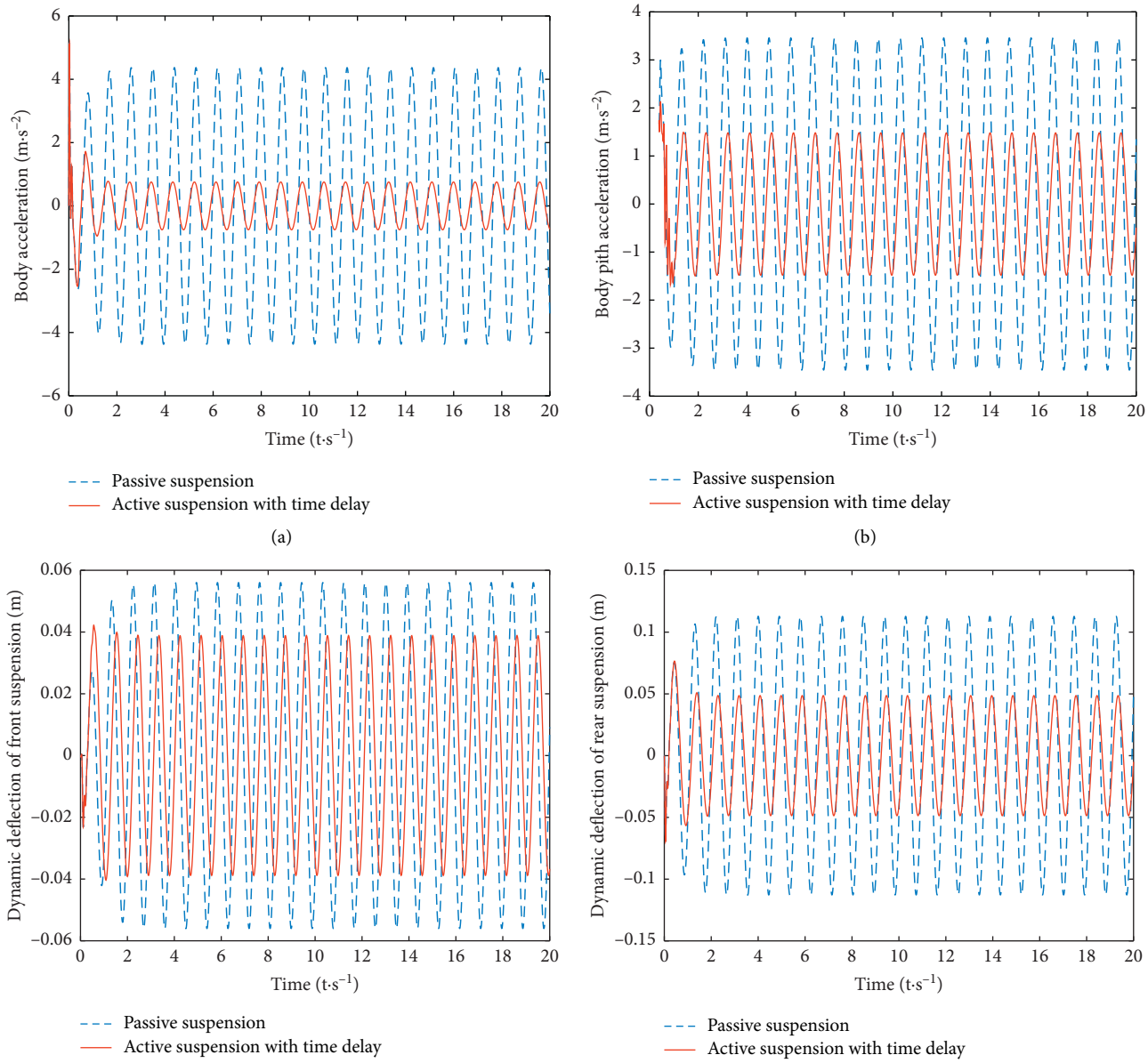

Figure 5: Continued.

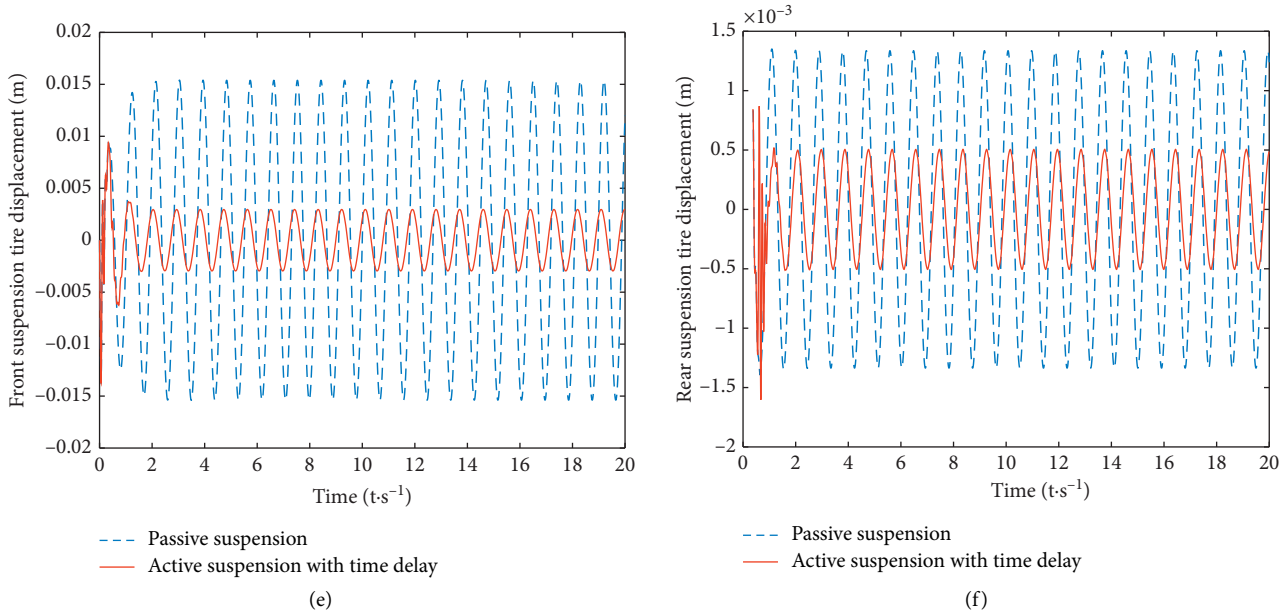

Figure 5: Simulation comparison of ride comfort index under harmonic excitation. (a) Body acceleration. (b) Body pitch acceleration. (c) Dynamic deflection of the front suspension. (d) Dynamic deflection of the rear suspension. (e) Front suspension tire displacement. (f) Rear suspension tire displacement.

Table 2: RMS value of ride comfort index under harmonic excitation.

Performance indicators	Passive suspension	Active suspension with time delay	Reduced proportion (%)
RMS acceleration of body centroid $(\mathrm{m}\cdot\mathrm{s}^{-2})$	3.0647	0.5026	−83.60
RMS acceleration of vehicle pitch $(\mathrm{rad.s}^{-2})$	2.3646	1.1162	−52.80
RMS of dynamic deflection of front suspension (m)	0.0383	0.0275	9.78
RMS of dynamic deflection of rear suspension (m)	0.0772	0.0362	28.20
RMS of dynamic displacement of front tire (m)	0.0108	0.0020	−81.48
RMS of dynamic displacement of the rear tire (m)	$9.7508e-4$	$3.3363e-4$	−68.78

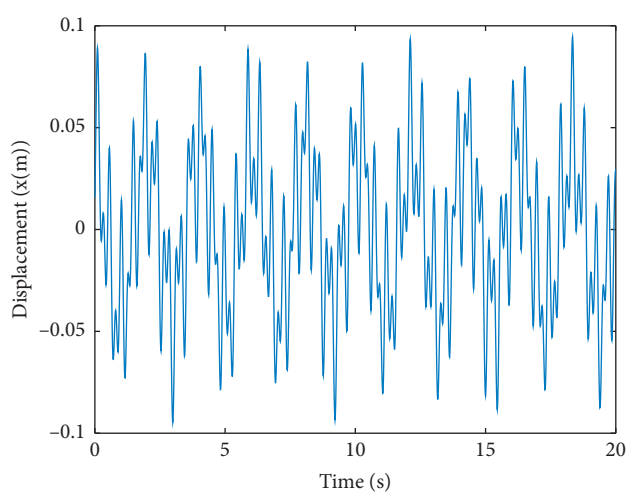

Figure 6: Disturbance change curve of random excitation displacement.

respectively, and the damping efficiency is 15.57% and 21.99%. This illustrates the active suspension pair with double time-delay feedback control. Both the body acceleration and pitch acceleration have been significantly optimized, which has greatly improved the ride comfort of the vehicle. Still, the ride comfort of the vehicle has increased

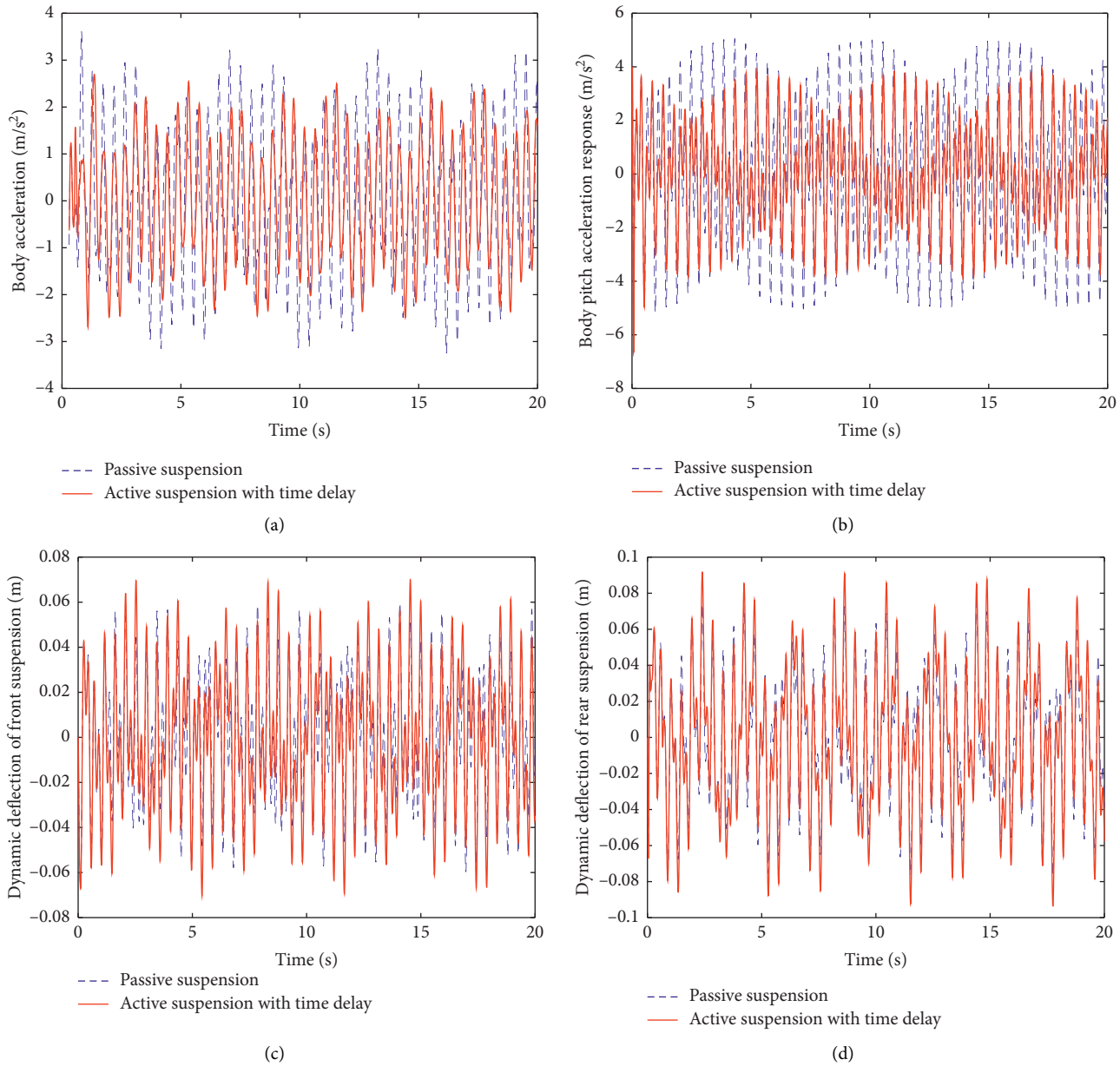

Figure 7: Continued.

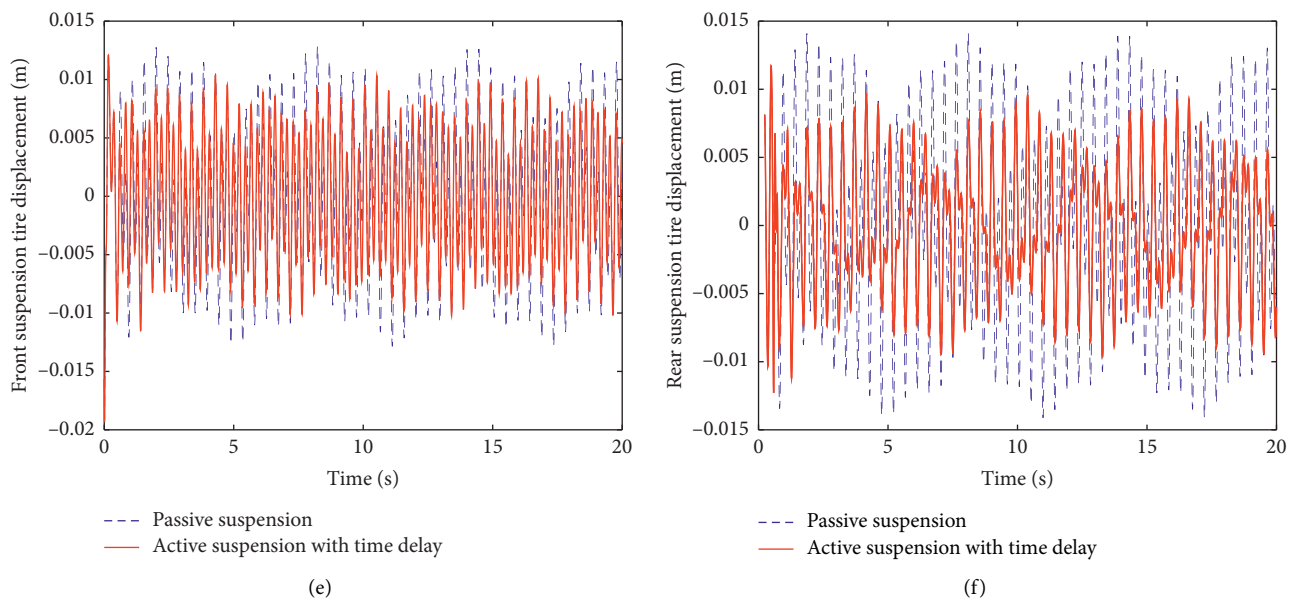

Figure 7: Simulation comparison of smoothness index under complex excitation. (a) Body acceleration. (b) Body pitch acceleration. (c) Dynamic deflection of the front suspension. (d) Dynamic deflection of the rear suspension. (e) Front suspension tire displacement. (f) Rear suspension tire displacement.

Table 3: RMS value of ride comfort index under random excitation.

Performance indicators	Passive suspension	Active suspension with time delay	Reduced proportion (%)
RMS acceleration of body centroid ($m \cdot s^{-2}$)	1.4898	1.2578	−15.57
RMS acceleration of vehicle pitch ($rad.s^{-2}$)	2.3858	1.8610	−21.99
RMS of dynamic deflection of front suspension (m)	0.0276	0.0303	9.78
RMS of dynamic deflection of rear suspension (m)	0.0341	0.0384	12.61
RMS of dynamic displacement of front tire (m)	0.0060	0.0055	−8.33
RMS of dynamic displacement of the rear tire (m)	0.0067	0.0047	−29.85

while the dynamic deflection of the front and rear suspensions has increased, as in Figures 7(c) and 7(d). The dynamic deflection of the front and rear suspensions has increased, and the root mean square values have increased from 0.0276 and 0.0341 to 0.0303 and 0.0384, but the increase is within the range of our design (± 100 mm), and the limit stroke of the dynamic deflection has not been exceeded. As in Figures 7(e) and 7(f), the corresponding root mean square values of the relative displacement of the front and rear tires have been reduced from 0.0060 and 0.0067 to 0.0055 and 0.0047, and the optimized efficiency is 8.33% and 29.85%. The passive suspension has also been reduced to a certain extent, indicating that double time-delay feedback control active suspension can significantly improve vehicle ride comfort and vehicle driving safety.

6. Conclusions

Under the premise of stability, this paper researches the damping effect of the active suspension system with double time-delay feedback control on the semicar model. Simulate the vibration characteristics of the vehicle under random excitation and harmonic excitation. Use the amplitude-frequency characteristic function as the objective function to obtain the time-delay feedback gain and time delay by particle swarm optimization and analyze the stability of the system to ensure the stability of the system. The below conclusions are obtained from the simulation and analyzing the semicar model with double time-delay feedback control.

(1) Aiming at the four-degree-of-freedom vehicle suspension system, use the time-delay dynamic shock absorber theory to bring in the front and rear double time-delay tire state feedback control and propose the frequency-domain scanning method to determine the stability of the double time-delay feedback control system.

(2) The center of mass acceleration and pitch acceleration of the vehicle body are improved significantly by using the active suspension with double time-delay feedback control under harmonic excitation and random excitation, which also improves the comfort and maneuverability of the vehicle significantly. Although the dynamic deflection of the front and rear suspensions increases under random excitation, the increasing range is within the design permission, and the dynamic displacement of the front and rear wheels is also clearly controlled to

ensure the grounding of the tires and the driving safety of the vehicle. The results show that the active suspension vehicle with double time-delay feedback control has a significant damping control effect, which can improve the vehicle's comfort and maneuverability very much.

Data Availability

The data used to support the findings of this study are included within the article.

Conflicts of Interest

The authors declare that there are no conflicts of interest regarding the publication of this paper.

Acknowledgments

This work was supported by the National Natural Science Foundation of China (Grant no. 51275280).

References

[1] J. D. J. Lozoya-Santos, R. Morales-Menendez, and R. A. Ramírez Mendoza, "Control of an automotive semi-active suspension," *Mathematical Problems in Engineering*, vol. 2012, pp. 1–21, 2012.

[2] L. Chen, R. C. Wang, H. B. Jiang, L. K. Zhou, and S. H. Wang, "Time delay on semi-active suspension and control system," *Chinese Journal of Mechanical Engineering*, vol. 42, no. 1, pp. 130–133, 2006.

[3] D. M. Zhang and L. Yu, "Review of stability analysis of linear time delay systems," *Control and Decision*, vol. 23, no. 8, pp. 841–849, 2008.

[4] W. Z. Zhang, B. Zhang, X. H. Wu, and Q. Sun, "Analysis of the influence of time delay on the control effect of active vibration control system," *China Mechanical Engineering*, vol. 24, no. 3, pp. 317–321, 2013.

[5] N. Olgac and R. Sipahi, "An exact method for the stability analysis of time-delayed linear time-invariant (LTI) systems," *IEEE Transactions on Automatic Control*, vol. 47, no. 5, pp. 793–797, 2002.

[6] N. Olgac and R. Sipahi, "The cluster treatment of characteristic roots and the neutral type time delayed systems," *Dynamic Systems and Control, Parts A and B*, vol. 127, no. 1, 2005.

[7] T. Vyhlídal, N. Olgac, and V. Kučera, "Delayed resonator with acceleration feedback - complete stability analysis by spectral methods and vibration absorber design," *Journal of Sound and Vibration*, vol. 333, no. 25, pp. 6781–6795, 2014.

[8] H. Y. Hu and Z. H. Wang, "Research progress in dynamics of controlled mechanical systems with time delay," *Progress in Natural Science*, vol. 10, no. 7, pp. 577–585, 2000.

[9] H. Y. Hu and Z. H. Wang, "Research progress of nonlinear time delay dynamical systems," *Mechanics Progress*, vol. 29, no. 4, pp. 501–512, 1999.

[10] H. Su and G. Y. Tang, "Vibration control of active suspension system with input delay," *Control Theory and Application*, vol. 33, no. 4, pp. 552–558, 2016.

[11] J. Zhang, H. Su, L. K. Wang, and G. Y. Tang, "Approximate optimal tracking control for discrete time systems with state and input delays," *Control and Decision*, vol. 32, no. 1, pp. 157–162, 2017.

[12] J. Xu and J. P. Li, *The Recent Research Progress and Prospect of Time Delay Systems Dynamics*, Springer, Berlin, Germany, 2006.

[13] Y. Y. Zhao and J. Xu, "Time delay dynamic vibration absorber and its influence on the vibration of main system," *Journal of Vibration Engineering*, vol. 19, no. 4, pp. 548–552, 2006.

[14] Y. Y. Zhao and R. M. Yang, "Saturation control of damping frequency band of self-parameter vibration system using time delay feedback control," *Acta Physica Sinica*, vol. 60, no. 10, p. 104304, 2011.

[15] N. A. Saeed, W. A. El-Ganini, and M. Eissa, "Nonlinear time delay saturation-based controller for suppression of nonlinear beam vibrations," *Applied Mathematical Modelling*, vol. 37, no. 20-21, pp. 8846–8864, 2013.

[16] N. A. Saeed and W. A. El-Ganaini, "Time-delayed control to suppress the nonlinear vibrations of a horizontally suspended Jeffcott-rotor system," *Applied Mathematical Modelling*, vol. 44, pp. 523–539, 2017.

[17] N. A. Saeed and W. A. El-Ganaini, "Utilizing time delays to quench the nonlinear vibrations of a two-degree-of-freedom system," *Meccanica*, vol. 52, no. 11-12, pp. 2969–2990, 2017.

[18] N. A. Saeed and H. A. El-Gohary, "Influences of time-delays on the performance of a controller based on the saturation phenomenon," *European Journal of Mechanics - A/Solids*, vol. 66, pp. 125–142, 2017.

[19] K. W. Wu, C. B. Ren, J. S. Cao, and Z. C. Sun, "Reach on damping control and stability analysis of vehicle with double time-delay and five degrees of freedom," *Journal of Low Frequency Noise, Vibration and Active Control*, 2020.

[20] W. Hu and L. I. Zhi-Shu, "A simpler and more effective particle swarm optimization algorithm," *Journal of Software*, vol. 18, no. 4, pp. 861–868, 2007.

[21] X. G. Li, *Several Studies on the Stability of Time Delay Systems*, Doctoral dissertation, Shanghai Jiao Tong University, Shanghai, China, 2007.

[22] W. Q. Fu, H. Pang, and K. Liu, "Modeling and stability analysis of semi-active suspension with time delay," *Journal of Mechanical Science and Technology*, vol. 18, no. 4, pp. 213–218, 2017.

[23] R. Sipahi and N. Olgac, "Kernel and offspring concepts for the stability robustness of multiple time delayed systems (MTDS)," *Journal of Dynamic Systems Measurement & Control*, vol. 129, no. 3, pp. 245–251, 2007.

[24] R. Sipahi and N. Olgac, "Stability robustness of retarded LTI systems with single delay and exhaustive determination of their imaginary spectra," *SIAM Journal on Control and Optimization*, vol. 45, no. 5, pp. 1680–1696, 2006.